Dynamic Properties of Surface Liquefied Site Silty-Sand of Tripura, India

Kunjari Mog(✉) and P. Anbazhagan

Department of Civil Engineering, Indian Institute of Science, Bangalore 560012, India
mogkunjari@gmail.com, anbazhagan@iisc.ac.in

Abstract. Due to increase in the rate of occurrence of earthquakes and associated damages, site-specific dynamic models are attracted to research in the recent past. The shear modulus degradation curve, damping characteristics and shear wave velocity profile are indispensable input properties required for carrying out the site response analysis. However, most of the site response studies are being carried out using existing dynamic model developed for generic soil. In the present study, results of resonant column and cyclic triaxial tests on reconstituted dry silty-sands specimens obtained from the recently liquefied site of Tripura, India is presented. The shear modulus degradation curve and damping ratio for a low ($<10^{-3}$) to high strain range (up to 5%) are presented and compared with the available well-known curves and discussed. Also, the effects of confining pressure and relative density on dynamic properties are presented. Further, comparison has been made between the shear wave velocity measured in the liquefied field using Multichannel Analysis of Surface Waves (MASW) and laboratory results of low strain shear wave velocity. These results can be used for amplification estimation or micro-zonation studies in Tripura.

Keywords: Shear modulus · Damping · Silty-sands · Resonant column
Cyclic triaxial · In-situ shear wave velocity

1 Introduction

Tripura state is in the north-eastern part of India and it is close to the Himalayan belt that is seismically very active due to the convergent boundary of Indian plate with Eurasian plate. The state falls in seismic zone V as per the Indian seismic code (IS: 1893 2016) with an anticipated zero period acceleration of 0.36 g. Recently, Tripura is jolted by a moderate magnitude of 5.7 (Mw) in the year 2017, January 3rd (USGS; Debbarma et al. 2017; Anbazhagan et al. 2017). The epicenter was traced at Ambassa, Dhalai district of Tripura, India. It brought the liquefaction at agricultural farm land that caused extensive damages to crop and developed numerous cracks in a number of dwellings. It also led the lateral spreading in the river bank at Kanchanbari, Kumarghat area. The Geophysics Division, NER, Shillong, reported that soil type in Tripura is generally consists of unconsolidated sediments of thickness about more than 250 m, comprise mainly sand and silty soils. The large variations of depth to bedrock and

© Springer Nature Switzerland AG 2019
D. Choudhury et al. (Eds.): GeoMEast 2018, SUCI, pp. 140–154, 2019.
https://doi.org/10.1007/978-3-030-01920-4_12

high-water table along with presence of soft silty sands dictate the preparation of seismic hazard maps, dynamic properties and liquefaction studies in Tripura.

Since early 1970's numerous significant researches come out on dynamic soil properties of soil by several researchers (Seed and Idriss 1970; Hardin and Drnevich 1972; Kokusho 1980; Woods 1991; Vucetic and Dobry 1991; Ishibashi and Zhang 1993; Zhang et al. 2005). Numerous model curves have been developed on shear modulus either on sands or clays although limited amount of work have been reported on gravelly soils or silty sands. The site-specific laboratory dynamic soil properties such as shear modulus and damping ratio are widely recognized as indispensible input parameters for carrying out the site-specific response analysis, liquefaction assessment, soil structure interaction, and seismic slope stability analysis. Similarly, geo-physical methods have become popular to geotechnical engineers to estimate the in-situ shear wave velocity (V_s) which in turns is used for site classification of soils, estimating the dynamic soil properties, liquefaction assessment, mapping the stratigraphic soil layers, detecting cavities or sinkholes and micro zonation studies or estimating the site-specific amplification estimation. The variation of V_s is dependent on soil density, soil type, effective stress, void ratio, depositional environment, etc. Most often the correlation between the Vs and SPT N values are used in places where geophysical measurement is not feasible or where the geophysical data is not available.

In the present study, dynamic properties and model of silty-sands is reported which had been emitted to the ground surface during 3rd January 2017 Tripura earthquake. The resonant column and cyclic triaxial tests have been conducted on the reconstituted soil samples of size 50 mm by 102 mm. The shear modulus degradation curve and damping ratio for a low ($<10^{-3}$) to high strain range (beyond 5%) are presented and compared with the available well-known curves and discussed. Further, the shear wave velocity measured in the liquefied field using Multichannel Analysis of Surface Waves (MASW) is compared with the laboratory (low strain) shear wave velocity.

2 Shear Modulus Degradation and Damping Curves

The experimental investigation was carried out on the surface liquefied soil obtained from the Kanchanbari, Tripura, India. Tripura state has experienced several moderate to big earthquakes in the past. Recently, an earthquake of magnitude Mw 5.7 hit the state on 3rd January 2017 which tremor was felt nearly all the north-eastern states of India including neighbouring country Bangladesh and Myanmar (Anbazhagan et al. 2017). Though the earthquake was of moderate magnitude, it caused the liquefaction in agricultural farmland in Kanchanbari, Tripura. It caused extensive damages to crop and developed numerous cracks in a number of houses. It also caused the lateral spreading in the river bank at Kanchanbari, Kumarghat area. The large variations of depth to bedrock and high-water table along with the presence of soft silty sands necessitate the preparation of seismic hazard maps, dynamic properties and liquefaction studies in Tripura.

The soil samples obtained from the site was sieved carefully and the grain size distribution curve is shown in Fig. 1. The basic property of soil was determined through laboratory test that is summarized in Table 1 (IS: 2720). Based on the Indian

Soil Classification System (IS: 2720), the soil can be classified as silty-sand. The undisturbed sample has been collected in a thin Shelby-tube sampler from a 3 m depth to measure the in-situ density and it is measured as 1.59 g/cc. The minimum and maximum relative density determined in the lab is 1.741 g/cc and 1.394 g/cc. The shear modulus degradation and damping curves for a low to high strain ranges are measured and curve has been generated. Further the effect of confining pressure and relative density on dynamic soil properties are discussed.

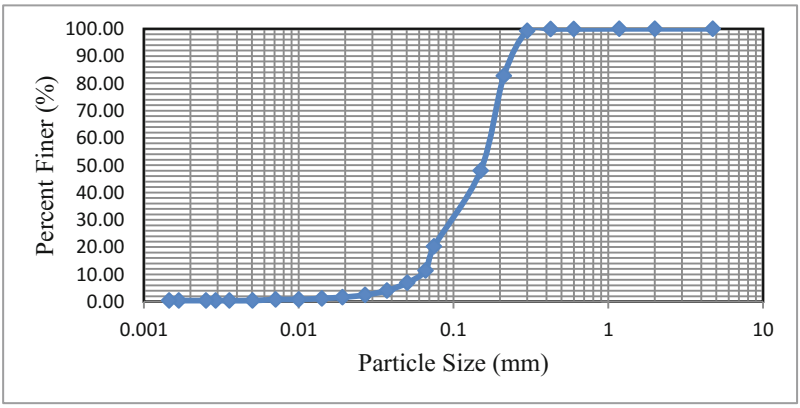

Fig. 1. Grain size distribution of tested soil

Table 1. Index properties of soil sample

Property	Value
Specific gravity, (G_s)	2.636
Particle size distribution	
(a) Gravel	0
(b) Fine Sand	79.753
(c) Silt & Clay	20.247
(d) Silt	19.837
(e) Clay	0.410
Uniformity coefficient (C_u)	2.903
Coefficient of Curvature (C_c)	0.861
Plastic limit	Non-plastic
Maximum dry unit weight, γ_{dmax}	1.741 g/cc
Minimum dry unit weight, γ_{dmin}	1.395 g/cc
Insitu dry density	1.66 g/cc
Indian standard classification	Silty-sand

2.1 Sample Preparation

A constant volume split mould of size 50.0 mm internal diameter and 102 mm height was used in preparing the test specimens. All the test specimens were prepared with a relative density of 80%, 50% and 30% using the dry tamping method reported by Ladd (1978). The same specimen preparation technique was adopted for both the resonant column and cyclic triaxial test. At first, an appropriate amount of air-dried representative sand was considered for preparing the test specimens. A latex rubber membrane was fixed to the bottom platen by securing it with O-rings. Next, the split mould was placed over the bottom platen, outside of the rubber membrane. The top part of the rubber membrane was strained and folded over the split mould. A constant vacuum of 15 to 30 kPa was applied through the bottom platen in order to remove the entrapped air between the membrane and the mould. The advantage of applying vacuum is that the membrane firmly sticks to the mould and it makes the sample stable during the preparation stage; also, it helps to reduce the sample disturbance while removing the mould. The sand was then gently poured into the split mould from a free drop height of 15 to 40 mm. The samples were prepared in six equal thick layers. Each layer was compacted using the tamping rod which weighs 142 g. In order to maintain a uniform density throughout the specimen height, the number of blows given to the lower layer was less compared to the successive upper layers. The volume of soil placed in each layer nearly corresponds to a 17 mm thick and the height of 102 mm was maintained varying the number of blows.

2.2 Resonant Column Test

Resonant Column (RC) instrument has been used widely in the laboratory for measuring the dynamic soil properties at low to medium strains (in either undisturbed or reconstituted states) as early as 1930's. Since then many different designed for resonant column devices have been developed and implemented by several researchers (Hardin and Richart 1963; Drnevich and Richart 1970; Stokoe et al. 1994) throughout the world. Three types of resonant column apparatus commonly available are fixed-fixed type, free-free and fixed-free type, based on the boundary conditions.

A Fixed-free GCTS resonant column device has been used in this study, where the soil column is fixed at the base and free to rotate at the top. A cylindrical soil specimen is excited at the top by an electromagnetic loading system or motor. A harmonic torsional excitation over a wide range of frequencies is applied at the top of the specimen to vibrate in one of its natural modes of vibration and the frequency response curve is drawn. The frequency, at which the amplitude is maximum, delineates the resonance frequency of the specimen. Once the resonance frequency is known, the shear wave velocity and corresponding shear modulus can be easily determined using the elasticity theory. The equation used to compute the maximum shear modulus is as follows:

$$G_{max} = \rho * V_{s^2} \tag{1}$$

Where: ρ = Density, V_s = Low strain shear wave velocity.

Initially, lower amplitude of torque was applied through a motor to the specimen and then the amplitude was gradually increased until the desired strain level is attained (0.01%). In the GCTS resonant column apparatus, the amplitude of the drive system or motor is applied in terms of percentage full scale (pfs) value that correlates the maximum output voltage. In addition, damping value is obtained from the recording of the free-vibration decay after the electromagnetic drive system was shut-off.

The resonant column tests were conducted on reconstituted cylindrical soil specimen of size 50 mm in diameter and 102 mm height. All the tests were conducted on the dry specimen. The relative density of 80%, 50% and 30% were considered for the resonant column test and the results obtained for the confining pressures of 50, 100, and 200 kPa are presented in the proceeding sections.

2.3 Cyclic Triaxial Test

After resonant column test is completed for the desired strain amplitude of 0.01%, the cell pressure from the triaxial chamber was released slowly and simultaneously the vacuum pressure of 15–20 kPa were applied to the soil specimen to keep the sample stand upright. Although small strains generated during the resonant column test would result in some rearrangement of the grains of soils in the dry specimen, however, it was found that the dry density has changed from the initial 1.48 g/cc to final 1.49 g/cc after the resonant column test as measured for 30% relative density test specimen and no change was observed for 80% and 50% relative density. Hence, changes in the relative density measured after the resonant column test remains nearly the same for 80% and 50% tests specimen except slight variation for the 30% test specimen. Therefore, keeping all the conditions (such as confining pressures, loading frequency etc.) same, next, cyclic triaxial tests were performed on the same specimen.

The instrument used for the cyclic triaxial test is servo-controlled that equipped with a load capacity of 10 kN pneumatic actuator. The system can perform both the strain controlled and stress-controlled tests with a frequency range of 0.01 Hz to 10 Hz. The different type of waveforms such as sine, triangular, square or any other type of random loading waveforms can be employed as an external input in the system. For the present study, the strain-controlled cyclic triaxial test was performed to determine the dynamic soil properties at medium to large strains. The double amplitude sinusoidal loading was applied for all cyclic triaxial tests at a loading frequency of 1 Hz. The load was applied through a low friction loading piston, the upper end to which a servo-controlled pneumatic actuator is fitted and the lower end is rigidly connected to the top of the specimen. The measurement of axial deformation, cell pressure, and pore water pressure for saturated specimen etc. can be made using a built-in data acquisition system. The output of cyclic triaxial tests is the plot of deviator stress (σ_d), versus axial strain (ε), also known as the hysteresis loop. A typical hysteresis loop for one cycle of loading is shown in Fig. 2 in which the slope of the secant line joining the extreme point is the dynamic Young's modulus, E. In the cyclic triaxial test, initially E is measured using $E = \sigma_d/\varepsilon$ and then shear modulus (G), shear strain (γ) are calculated from the following relationship:

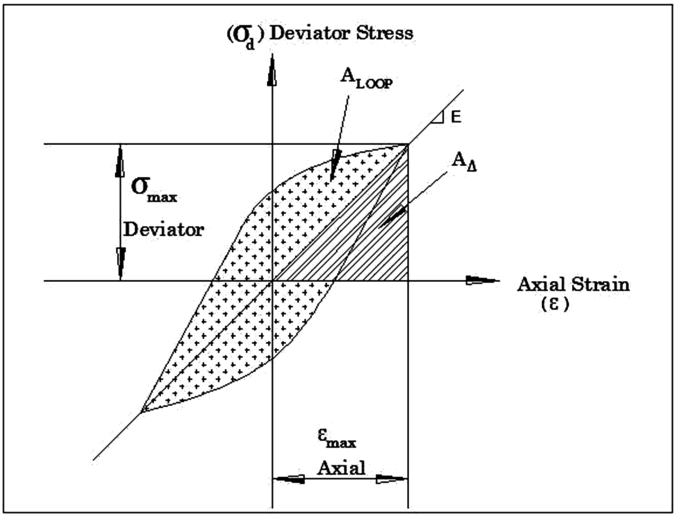

Fig. 2. Hysteretic stress-strain behaviour for one cycle of loading

$$G = E/2(1+\mu) \quad \text{and} \quad \gamma = (1+\mu)\varepsilon \tag{2}$$

Where: μ = Poisson's ratio. The μ value may be assumed as 0.4 for dry sand specimens as recommended by Silver and Park (1975).

The damping ratio D is a measure of the dissipated energy to the elastic strain energy (Kramer 1996), and it can be estimated from the area of hysteresis loop using the given equation:

$$D = \frac{A_{loop}}{4\pi A_{\Delta}} \tag{3}$$

Where, A_{loop} = Area enclosed by the hysteresis loop and A_{Δ} = Area of the triangle. Dynamic soil properties of large shear strains were obtained using a series of strain-controlled cyclic triaxial. The damping properties using both the conventional formula as given in Eq. 3 and modified asymmetrical hysteresis loop method as suggested by Kumar et al. (2017) as given in Eq. 4 is calculated and the variation between the two was found to be approximately 20 to 40% for the tested silty-sand samples. However, the damping ratio calculated using the Eq. 3 is reported in the present study. The modified damping estimation equation considering the asymmetrical hysteresis loop is given below and more details can be found in Kumar et al. (2017):

$$D^{\#} = \frac{A_{loop}}{\pi(A_{\Delta 1} + A_{\Delta 2} + A_{\square})} \tag{4}$$

Where $D^{\#}$ = Damping ratio by modified method, A_{loop} = Area enclosed by the hysteresis loop and $A_{\Delta 1} + A_{\Delta 2}$ = Area of the two triangles, $A_{\square}$ = Area of rectangle.

2.4 Effect of Confining Pressure on the Shear Modulus and Damping Properties at Large Shear Strain (Beyond 5%)

The resonant column and cyclic triaxial (strain controlled) tests were carried out to investigate the influence of confining pressure on dynamic properties of dry silty-sands. The variation of shear modulus with the shear strain at low ($<10^{-3}$) to high strain range (more than 5%) for the dry silty-sands tested at three different confining pressures (50, 100, 200 kPa) are shown in Fig. 3. The relative density considered for testing the soil specimen was 80%. From the Fig. 3 it can be observed that the confining pressure has a significant influence on shear modulus. The shear modulus (G) decreases with the increase in shear strain and G increases with the increase in confining stress. A noticeable variation in the value of shear modulus was observed for all the three different confining pressures (strain range 0.0001 to 1%), however, beyond 1% of shear strain, it follows the converging trends regardless of any confining pressures to which the soil specimens are subjected. The similar converging trends of the shear modulus (beyond 1%) has also been reported in the literature (Sitharam et al. 2008).

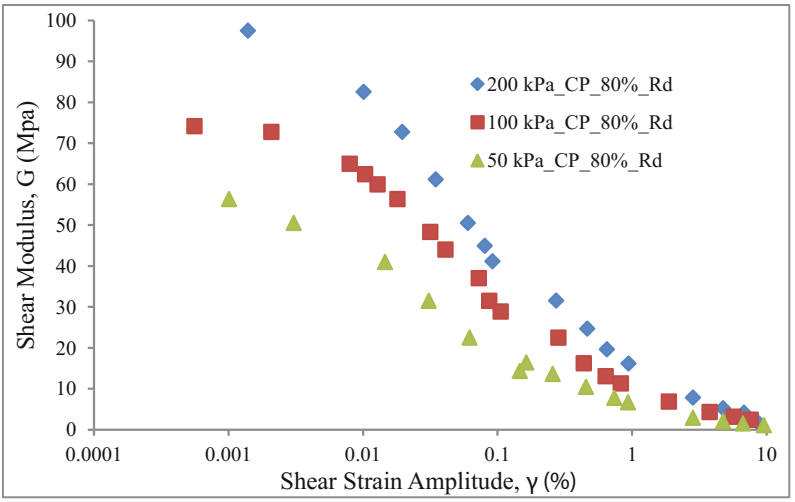

Fig. 3. Effect of confining pressures on shear modulus for a large shear strain

The influence of confining pressures on damping ratio is shown in Fig. 4. It can be observed from the figure that the damping ratio increases with the increase in shear strain amplitude for a given confining pressure. The damping ratio is observed to be maximum for a lower confining pressure (50 kPa) compared to that of higher confinement (100 kPa and 200 kPa). It can also be seen that the damping ratio is nearly equal up to a shear strain of 0.01%, however, beyond that strain level damping ratio decreases with the increase in confining pressures. It is also evident from the Fig. 4 that up to a shear strain of about 2%, the damping shows the conventional behavior of increasing trend with increasing shear strains, however, the decreasing trends of damping is noticeable beyond 2% of shear strain for all the three different confining

pressures. This decrement of damping at higher strains differs from the conventional trends (Damping increases or became asymptotic with increasing shear strains, beyond 1%) and is concords with the findings of Kumar et al. (2017).

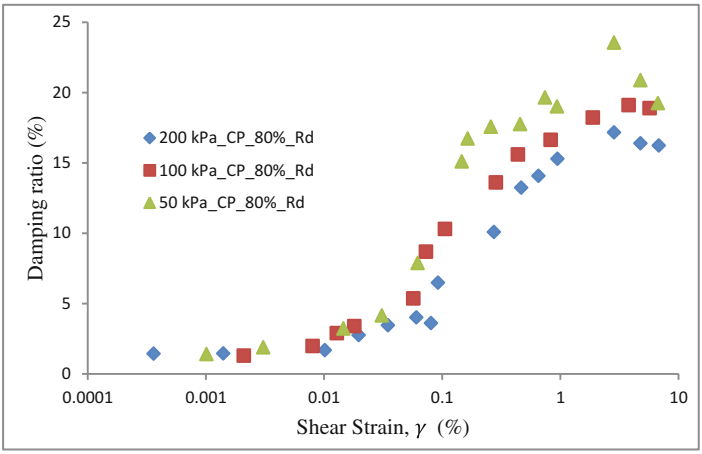

Fig. 4. Effect of confining pressures on damping ratio for a large shear strain

It is to be noted here that most of the damping curves reported in the literature are for the shear strain of less than 1% (Seed and Idriss 1970; EPRI 1993; Roblee and Chiou 2004) and beyond 1% of strain level the damping value is extrapolated or predicted (Kumar et al. 2017). The existing commercial software for dynamic analysis such as FLAC, SHAKE, and DEEPSOIL etc. also uses the same extrapolated conventional damping ratio curve. Hence, from the present study, it can be stated that conventional trends of damping ratio curve may not be appropriate to use in the geotechnical analysis for a wide strain range and it should consider the decreasing trends of damping behavior at large shear strain as shown in the Fig. 4.

2.5 Effect of Relative Density on Shear Modulus and Damping at Large Strain

The effect of relative density on shear modulus for a wide range of shear strain was investigated by performing RC and Cyclic Triaxial tests at three different relative densities such as 80%, 50%, and 30% respectively. The shear modulus variations with the shear strain with different relative densities are shown in Fig. 5. The result is shown for the confining pressure of 200 kPa. It is evident from the Fig. 5 that the shear modulus decreases with the decrease in relative density (80%, 50%, and 30%) up to a strain level of 0.5% and beyond that no variation in shear modulus is found. Hence, this clearly indicates that relative density has considerable influence on small strain shear modulus of silty-sands (less than 0.5%); however, it does not have an influence on large strain shear modulus at 200 kPa confining pressure.

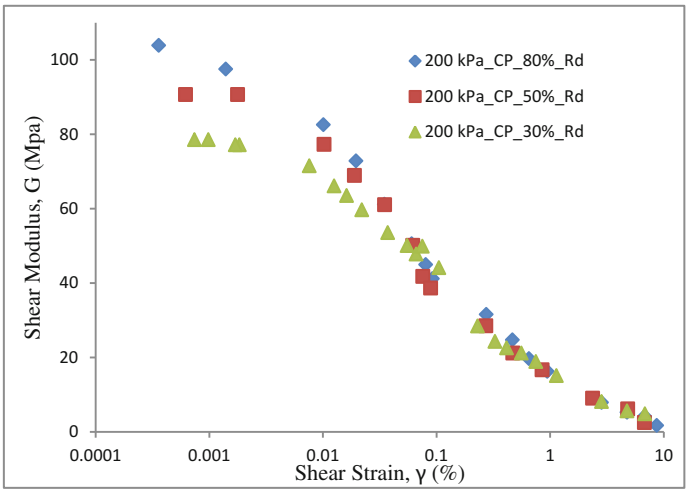

Fig. 5. Effect of relative density on shear modulus at 200 kPa confining pressure

Figure 6 shows the effect of relative density on damping ratio for a wide strain range. The dry silty-sand specimen was subjected to 200 kPa confining pressure for the relative density of 80%, 50% and 30% respectively. From the Fig. 6 it can be clearly observed that the relative density has negligible or no influences on damping ratio at various strain levels (Sitharam et al. 2008); only a slight variation in damping ratio is observed beyond 2% of shear strain in the present study.

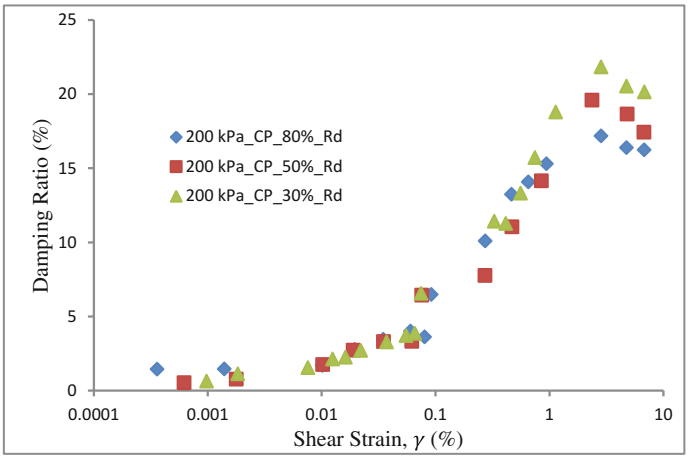

Fig. 6. Effect of relative density on damping ratio at 200 kPa confining pressure

2.6 Normalized Shear Modulus and Damping Curves

It is a general trend to represent the variation of shear modulus with respect to shear strain in terms of normalized shear modulus degradation curves. This normalized curve is then used for site response analysis or amplification estimation. The normalized shear modulus degradation curve for the silty-sand tested for different relative density (80%, 50%, 30%) for different confining pressures (200, 100, 50 kPa) is presented in Fig. 7 and the results is compared with the available well-known curves of sand. It can be observed from the Fig. 7 that the shear modulus obtained from the combined resonant column and cyclic tri-axial tests for silty-sands do not fit well within the upper and lower boundary range as proposed by Seed and Idriss (1970) for sands. However, the curvilinear shape or trend of normalized (G/G_{max}) curve is same as that of sand. Further, this normalized curve is compared with the other available curves for sands (EPRI 1993; Roblee and Chiou 2004) and shown in Fig. 7. The data presented in the present study exceeds the upper limit of Seed & Idriss curve and so as the case for other available curves as mentioned. This clearly brings about the fact that the presence of fines content caused the cyclic shearing strength to increase and the shear modulus of silty-sand show the higher value than the shear modulus of sands.

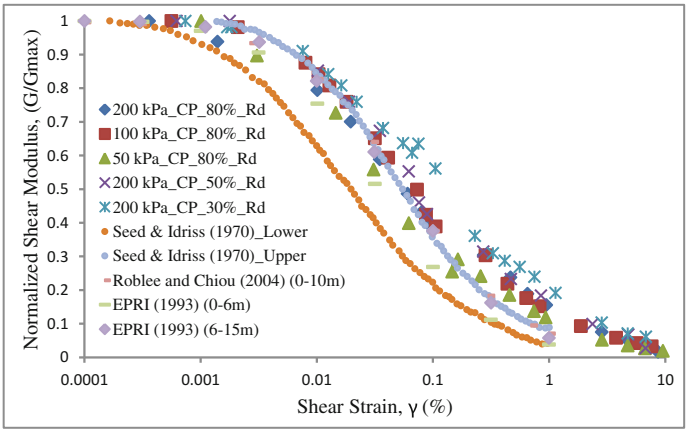

Fig. 7. Normalized shear modulus curve of silty-sands obtained from combined resonant column and cyclic triaxial test compared with sands

Also, as can be seen from the Fig. 8 that the range of damping for the present study falls much lower side from the lower bound curve of proposed Seed and Idriss (1970), EPRI (1993), Roblee and Chiou (2004) curve for sands. Based on the observed data, it can be concluded that strain-dependent shear modulus ratio of silty-sands is higher than that of sands and damping properties is lower than sands. The site specific dynamic shear modulus reduction curves developed from the present study could be used for site response studies or amplification estimation in the area. However, as the damping ratio curves for dry and saturated cohesionless soils are not the same at high strains

(Kumar et al. 2017), hence, the damping ratio curves as reported in the present study may be further studied for statured condition and can be used for the dynamic analysis.

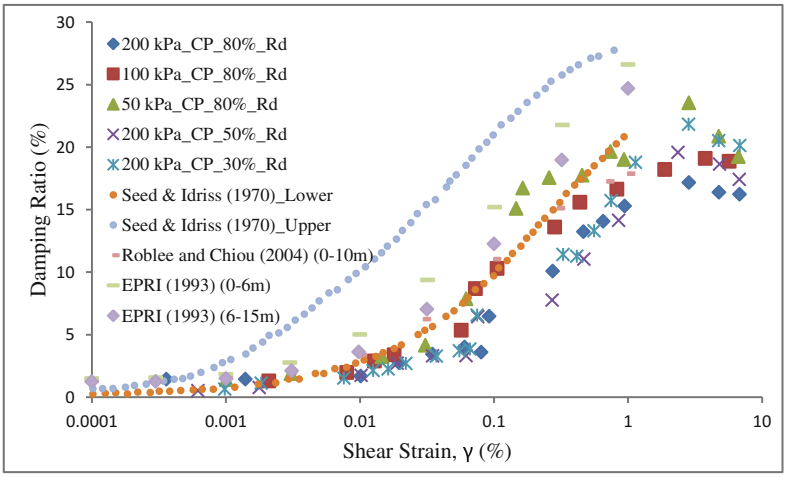

Fig. 8. Damping curve of silty-sands obtained from combined resonant column and cyclic triaxial test compared with sands

3 Field Measurement of V_s and Comparison with Laboratory V_s

The measurement of in-situ shear wave velocity and the comparison between the in-situ V_s and laboratory V_s is reported in this section. It is widely recognized fact that shear wave velocity profile is fundamental input parameter required in micro-zonation studies or in estimating the site-dependent amplification factor. The five sets of Multichannel Analysis of Surface Wave (MASW) tests were conducted at the liquefied site to measure the V_s and the average V_s has been considered to compare with laboratory V_s.

3.1 In-situ Measurement of Shear Wave Velocity

The geophysical methods have become popular among the geotechnical engineers and researchers to estimate the in-situ shear wave velocity (V_s) in the earthquake-prone areas. Various methods presently available to measure the V_s includes Spectral Analysis of Surface Wave (SASW) tests, Multichannel Analysis of Surface Wave (MASW) Tests, suspension logging tests, cross-hole or down-hole tests (Kramer 1996). Both the cross-hole and down-hole methods use body waves to estimate the shear wave velocity and data obtained from these measurements are fairly accurate. Though the cross-hole test requires drilling of minimum two boreholes and down-hole or up-hole test can be performed in a single boring, often the cost and time associated with these methods are huge; also, drilling of boreholes in urban areas often needs approval from the concerned authority and often drilling is not feasible in some areas. To alternate,

these destructive methods, non-destructive SASW or MASW test is preferred. The SASW and MASW test is the well-recognized technique which uses the Rayleigh waves for estimating the in-situ shear wave velocity.

In the present study, the MASW test has been conducted at the liquefied site of Kanchanbari, Tripura, India. The test method involves field testing and data processing which includes dispersion estimation and inversion. First, the 24 geophones with a minimum frequency of 2 Hz are placed in a linear arrangement at an equal interval of 2 m spacing. Then all the geophones are linked to the multichannel recorder. Next, a sledgehammer of 7.8 kg is dropped at one end of geophone line from a certain height to hit the 300 mm × 300 mm metal plate having 25 mm thickness which produces the vibration at the ground. Due to this vibration, the surface wave travels from the first geophone to the last geophone and data is recorded. The SurfSeis software has been used for processing the recorded data. The results obtained from the MASW test is presented in terms of variation of shear wave velocity with depth as shown in Fig. 9. It can be observed from the Fig. 9 that the shear wave velocity is in the range of 88 m/s to 228 m/s for the depth of 0.5 m to 12.5 m, which indicates that the stiffness beneath the ground surface at the site is soft or medium.

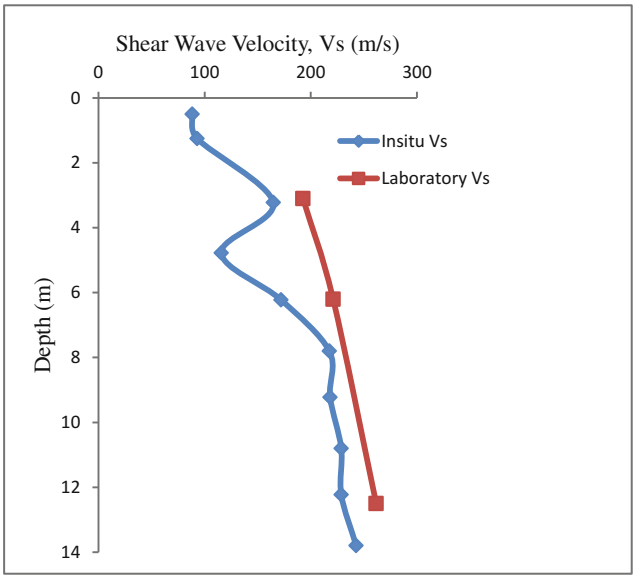

Fig. 9. Comparison of in-situ and laboratory shear wave velocity with depth

To compare the in-situ V_s with laboratory V_s, the reconstituted soil specimen prepared at 80% relative density which is close to the in-situ dry density (1.66 g/cc) at the site has been used and the result is shown in Fig. 9. The in-situ dry density was measured by extracting the partially undisturbed tube sample obtained from a depth of

3 to 3.5 m that was directly brought to the lab from the liquefied site. It can be observed from Fig. 9 that the low patches of shear wave velocities of depths at less than 7 m (or 3.5 to 5 m) is indicative of the possible in-situ liquefaction zones. However, it is amply clear that the laboratory results at these depths are noticeably higher than in-situ observation; the reason being once the site gets liquefied, and the pore-water is dissipated, a significant rearrangement of the cohesionless soil grains occurs, which generates a different void ratio, relative density and stress-state of the soil. Under such condition, it is primarily a different soil state than that present before liquefaction. The small-strain shear modulus, Gmax, and thus, Vs, depends largely on the above-mentioned parameters (Kramer 1996; Ishibashi and Zhang 1993). It can also be seen that the stress state beyond 8 m depth is noticeably same possibly due to the non-liquefied medium, and hence, the results are in good agreement from depths 8 m–12.5 m. Though the V_s profile is available for the deeper depth, however, since the laboratory tests have been conducted up to a confining pressure of 200 kPa which represents the 12.5 m depth from the ground surface, the comparison between the two has been shown up to the same depth.

4 Conclusions

The paper presented the development of site-specific shear modulus and damping ratio curved through the laboratory and in-situ experimental investigation. Dry silty-sand samples obtained from the liquefied site of Trippura, India were subjected to resonant column and cyclic triaxial tests to develop the dynamic properties over varying strain range. MASW tests have also been conducted at the field to obtain the variation of shear wave velocity with depth, and comparative results of the laboratory and in-situ tests have been provided.

The shear modulus of the silty-sand is found to be affected significantly by the variations of confining pressures (at small to large strain range) and relative density (at small strains). However, the damping ratio exhibits no influence over the variations of the relative density. The damping properties show the conventional behavior of increasing trend with increasing shear strains; however, the decreasing trends of damping is observed beyond 2% of shear strain for all the confining pressures to which the samples are subjected. This reduction of damping ratio at higher strains (beyond 2%) differs from the conventional extrapolated trends and should be carefully considered while using the site response analysis or other dynamic analysis.

The normalized shear modulus ratio compared with the available well-known curves for sands revealed the fact that silty-sands exhibits higher modulus ratio than that of sands and exactly opposite trends is observed in case of damping ratio. Based on the present study it can also be interpreted that the possible liquefied layer was at the depth of 3.5 to 5 m for the liquefied site of Kanchanbari, Tripura, India, which has the V_s value less than 150 m/s.

Acknowledgment. The authors thank the Board of Research in Nuclear Sciences (BRNS) of the Department of Atomic Energy (Dae), Government of India for funding the project titled "Probabilistic seismic hazard analysis of Vizag and Tarapur considering regional uncertainties", Ref: BRNS/36016-2016.

References

Anbazhagan, P., Sitharam, T.G.: Evaluation of dynamic properties and ground profiles using MASW: correlation between Vs and N 60. In: Proceedings of 13th Symposium on Earthquake Engineering, Indian Institute of Technology, Roorkee, December 2006, pp. 18–20 (2006)

Anbazhagan, P., Mog, K., Reddy, G.R.: Liquefaction in Kanchanbari Tripura, India due to Moderate Magnitude Earthquake. Current Science (Under review) (2017)

Debbarma, J., Martin, S.S., Suresh, G., Ahsan, A., Gahalaut, V.K.: Preliminary observations from the 3 January 2017, MW 5.6 Manu, Tripura (India) earthquake. J. Asian Earth Sci. **148**, 173–180 (2017)

GCTS-CATS: Resonant column & torsional shear test. User Guide & Ref 1.97:1-143 (2007)

Seed, H.B., Idriss, I.M.: Soil Moduli and Damping Factors for Dynamic Response Analyses. Report No. EERC 70-10, University of California, Berkeley, December 1970. Also Section 5, Soil Behavior Under Earthquake Loading Conditions, Report to U.S. Atomic Energy Commission, SW-AA (1972)

Hanumantharao, C., Ramana, G.V.: Dynamic soil properties for microzonation of Delhi, India. J. Earth Syst. Sci. **117**(2), 719–730 (2008)

Hardin, B.O., Drnevich, V.P.: Shear modulus and damping in soils: design equations and curves. J. Soil Mech. Found. Div. **98**(sm7) (1972)

Imai, T., Yoshimura, M.: The relation of mechanical properties of soils to P and S wave velocities for soil ground in Japan. Urana Research Institute, OYO Corp. (1972)

IS: 1893 (Part 1): Criteria for earthquake resistant design of structures – Part 1: General provisions and buildings; Bureau of Indian Standards, New Delhi (2016)

IS: 2720 (Part 14): Methods of test for soils: Determination of density index (Relative Density) of cohesionless soils. Bureau of Indian Standards (BIS), New Delhi (1986)

IS: 2720 (Part 3): Methods of test for soils: determination of specific gravity. Bureau of Indian Standards (BIS), New Delhi (1980)

IS: 2720 (Part 4): Methods of test for soils: Grain size analysis. Bureau of Indian Standards (BIS), New Delhi (1983)

Ishibashi, I., Zhang, X.: Unified dynamic shear moduli and damping ratios of sand and clay. Soils Found. **33**(1), 182–191 (1993)

Jafari, M.K., Shafiee, A., Razmkhah, A.: Dynamic properties of fine grained soils in south of Tehran. J. Seismol. Earthq. Eng. **4**(1), 25 (2002)

Kokusho, T.: Cyclic triaxial test of dynamic soil properties for wide strain range. Soils Found. **20** (2), 45–60 (1980)

Kramer, S.: L.(1996). Geotechnical Earthquake Engineering. Pren-tice Hall, New Jersey (2005)

Kumar, S.S., Krishna, A.M., Dey, A.: Evaluation of dynamic properties of sandy soil at high cyclic strains. Soil Dyn. Earthq. Eng. **99**, 157–167 (2017)

Ladd, R.S.: Preparing test specimens using undercompaction. Geotech. Test. J. **1**(1), 16–23 (1978)

Maheshwari, B.K., Mahajan, A.K., Sharma, M.L., Paul, D.K., Kaynia, A.M., Lindholm, C.: Relationship between shear velocity and SPT resistance for sandy soils in the Ganga basin. Int. J. Geotech. Eng. **7**(1), 63–70 (2013)

Rollins, K.M., Diehl, N.B., Weaver, T.J.: Implications of Vs-BPT (N 1) 6 0 correlations for liquefaction assessment in gravels. In: Geotechnical Earthquake Engineering and Soil Dynamics III, pp. 506–517. ASCE (1998)

Silver, M.L., Park, T.K.: Testing procedure effects on dynamic soil behavior. J. Geotech. Geoenviron. Eng. **101**(ASCE# 11671 Proceeding) (1975)

Sitharam, T.G., Ravishankar, B.V., Vinod, J.S.: Dynamic properties of dry sands. Indian Geotech. J. **38**(3), 334–344 (2008)

Sykora, D.W., Koester, J.P.: Correlations between dynamic shear resistance and standard penetration resistance in soils. In: Earthquake Engineering and Soil Dynamics II—Recent Advances in Ground-Motion Evaluation, pp. 389–404. ASCE, June 1988

United State Geological Survey (USGS), 3rd January 2017, M 5.7 – 20 km ENE of Ambassa, India

Vucetic, M., Dobry, R.: Effect of soil plasticity on cyclic response. J. Geotech. Eng. **117**(1), 89–107 (1991)

Woods, R.D.: Field and laboratory determination of soil properties at low and high strains (1991)

Zhang, J., Andrus, R.D., Juang, C.H.: Normalized shear modulus and material damping ratio relationships. J. Geotech. Geoenviron. Eng. **131**(4), 453–464 (2005)